EAI Endorsed Transactions
on Digital Transformation of Industrial Processes Research Article EAI.EU

# Regression analysis of the effect of Ge and Si on the torsional strength and fracture angle of aluminium alloys using one-way ANOVA

Sarvar Tursunbaev [1,*], Umidjon Mardonov [1], Nigora Rizaeva[1], Nuritdin Tadjiev[1] and Nargiza Mahkmudova[1]

[1]Tashkent state technical university, 100095, Tashkent, Uzbekistan

## Abstract

INTRODUCTION: Aluminium alloys represent a highly sought-after category of structural materials, ranking just below iron-carbon alloys in their application within the manufacturing sector. In this study, the effect of germanium as an oxide (GeO2) form and Si, introduced as modifying additives into aluminium casting alloys on their torsional strength was investigated.
OBJECTIVES: Aluminium alloys ZL201 and AA5056 were selected as a study objective which are widely used in the production of shaped castings.
METHODS: During the study, germanium as an oxide (GeO2) form and silicon were introduced into the composition of selected aluminium alloy grades in various combinations, after which their torsional strength was tested using WP 500 testing equipment. Specimens melted in an induction furnace and cast at 720 °C into sand-clay moulds. The moulds were prepared as standardized specimens. During the study, the torsional failure angle and torsional strength of the aluminium specimens were determined. These parameters were calculated using a computer program linked to the WP 500 testing equipment. The effect of adding germanium and silicon on torsional strength and fracture angle of ZL201 and AA5056 aluminium alloys was investigated. One-way ANOVA was used to verify the reliability of the experimental tests.
RESULTS: It was found that the torsional strength of the alloy increased under the influence of germanium and silicon; however, when the germanium content exceeded 2%, the torsional strength of the studied aluminium alloys decreased. Based on the obtained results, graphs of the fracture angle and torsional strength as a function of the germanium and silicon content in the alloy were constructed.
CONCLUSION: Obtained results demonstrated that the addition of GeO2 with Si led to significant grain refinement, dispersion of eutectic and intermetallic phases, and improvement in structural homogeneity. The findings highlight the existence of a well-defined optimal Ge% concentration around 2%, at which both frictional and mechanical properties are maximized.

**Keywords:** strength, aluminium alloy, predictive analytics, modification, silicon, germanium, one-way ANOVA

Received on 17 February 2026, accepted on 27 May 2026, published on 04 June 2026

Copyright © 2026 Sarvar Tursunbaev *et al.*, licensed to EAI. This is an open access article distributed under the terms of the CC BY-NC-SA 4.0, which permits copying, redistributing, remixing, transformation, and building upon the material in any medium so long as the original work is properly cited.

doi: 10.4108/dtip.11974

## 1. Introduction

Aluminium casting alloys are currently one of the most in-demand groups of structural materials, second only to iron-carbon alloys in terms of their use in the mechanical engineering industry [1–5]. Current research is aimed at improving the performance and mechanical properties of aluminium alloys by introducing various alloying and

*Corresponding author. Email: anvarovichsarvar908@gmail.com

modifying elements. Numerous experimental and theoretical studies have been conducted in this area by domestic and international researchers [6–9].

For example, Wei Li and co-authors studied the effect of adding small amounts of germanium (Ge) to AA5056 aluminum alloy on its microstructure and mechanical properties. It was found that cracks and defective phases can form during the normal rapid cooling of AA5056 alloy. The introduction of 0.05–0.2% germanium contributed to the formation of finely dispersed and uniformly distributed particles, reduced sensitivity to cooling, and increased strength, high-pressure resistance, and stress resistance [10]. M. Victoria and co-authors investigated the accelerated crystallization of Al–Cu aluminum alloys alloyed with small amounts of silicon (Si) and germanium (Ge), introduced at 8% plastic deformation before artificial aging. Using transmission electron microscopy, the mechanism of accelerated crystal formation was studied in detail. It was found that plastic deformation increases the rate of Si–Ge crystal formation, leading to an increase in their bulk density and, consequently, to an increase in the strength of Al–Cu alloys [11].

In the works of I. N. Ganiev and co-authors, it was shown that the combined introduction of germanium and strontium into AK9M2 aluminium alloy under vacuum conditions significantly improves its mechanical properties [12]. Despite existing research, the effect of germanium and silicon, combined as modifying elements in aluminium under open atmosphere conditions, on torsional strength remains poorly understood.

Despite the above-mentioned studies, the effect of modifying elements on torsional strength has not been sufficiently investigated. In particular, the influence of the amount of modifying elements added to aluminium alloys on their torsional strength has not been studied. In this paper, the authors investigate the effect of germanium (Ge) and silicon (Si), introduced as modifying additives into the ZL201 and AA5056 aluminium alloys, on their torsional strength.

## 2. Materials and methods

### 2.1. Materials

During operation, mechanical engineering components are sometimes subjected to shear loads alone, which can cause sections to shift, slide, or crack, resulting in shear deformation. Shear deformation occurs when a prismatic beam is subjected to two opposing forces at very close proximity in the transverse direction. When a beam is torsionally twisted, only one internal force factor—the torque Mb—is generated in its cross-sections. When a beam with a circular cross-section is torsionally twisted, its length remains unchanged. The beam's cross-sectional surface, which was flat before deformation, remains flat after deformation. In this case, only one section rotates at an angle relative to the other. From this, it can be concluded that when torsion occurs, a beam with a circular cross-section experiences pure shear deformation. In the transverse and longitudinal sections of a beam with a circular cross-section, only shear stresses are generated under the action of the torque. In a plane that forms an angle of 45° with the longitudinal axis of the beam, only normal (principal) stresses act [13, 14].

Aluminium alloys ZL201 and AA5056 were selected for the experiments. The chemical composition of these alloys is given in Tables 1.

Table 1. Chemical composition of ZL201 and AA5056 aluminium alloy (%)

| ZL201 | | | | | | | | | |
|---|---|---|---|---|---|---|---|---|---|
| № | Fe | Si | Mn | Ti | Al | Cu | Zr | Mg | Zn |
| 1 | <0.2 | <0.3 | 0.6-1 | 0.15-0.35 | 92.45-94.75 | 4.5-5.3 | <0.2 | <0.05 | <0.2 |
| **AA5056** | | | | | | | | | |
| № | Fe | Si | Mn | Al | Cu | Zr | Mg | Zn | Impurities (total) |
| 1 | <1.5 | 1.3 | 0.1-0.4 | 91-94.6 | <0.1 | <0.15 | 4.5-5.5 | <0.2 | <1.8 |

### 2.2. Experimental setup

To determine the torsional strength, the samples were poured into sand-clay molds at a temperature of 720 ºC in an induction furnace [15]. The resulting aluminium alloys are shown in Fig. 1.

The cast specimens were machined according to the DIN standard and had a diameter of Ø 6 mm and a length of 115 mm [16]. An image of the machined specimens is shown in Fig. 2.

**Figure 1.** Specimens cast for torsion testing

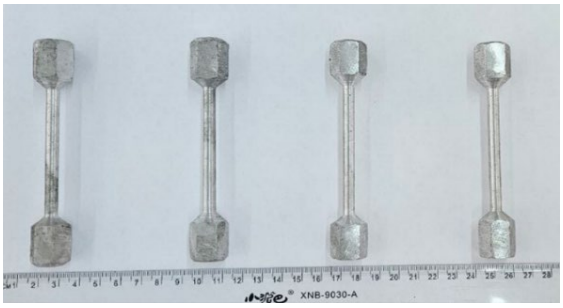

**Figure 2.** Machined samples

Experimental tests were conducted using the WP 500 testing equipment (Fig. 3). The WP 500 is designed to determine the torsional strength of rods made of aluminium alloys. It measures the torque and torsion angle [17]. The testing process is shown in Fig. 4.

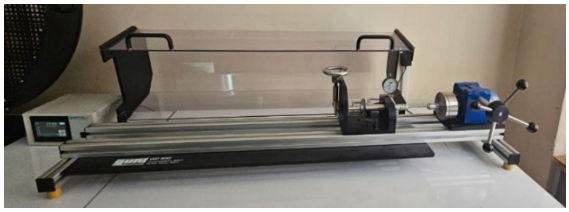

**Figure 3.** WP 500 test equipment

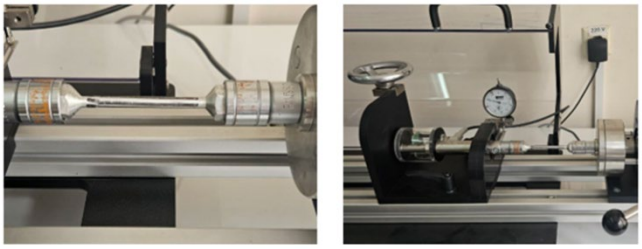

**Figure 4.** The process of testing for torsion

In the experimentations, the samples were subjected to twisting at specific angles, resulting in their failure (Fig. 5). Based on the data obtained using a computer connected to the device, the strength limits were calculated using the following formula [18].

$$\tau_B = \frac{M_b}{W_p} = \frac{16M_b}{\pi d^3}. \quad (1)$$

**Figure 5.** Condition of samples after testing

## 3. Results and Discussions

### 3.1. Torsional Performance

Using the formula above, the torsional strength "$\tau_B$" for aluminium alloys was determined. The results obtained from the torsion tests are presented in Table 2. Based on these data, a graph was constructed showing the relationship between the germanium content in the aluminium alloy and the torque and fracture angle (Fig. 6 and 7).

Table 2. Results of experiments

| Al composition | Fracture angle, $\varphi$ | Torsional strength, $\tau_B$ |
|---|---|---|
| **AA5056** | 32.5 | 125.0 |
| AA5056-1%Ge-5%Si | 24.5 | 126.2 |
| AA5056-2%Ge-5%Si | 49 | 134.9 |
| AA5056-3%Ge-5%Si | 46 | 129.7 |
| **ZL201** | 42 | 150.9 |
| ZL201-1%Ge-5%Si | 44 | 158.1 |
| ZL201-2%Ge-5%Si | 68 | 175.7 |
| ZL201-3%Ge-5%Si | 41 | 145.1 |

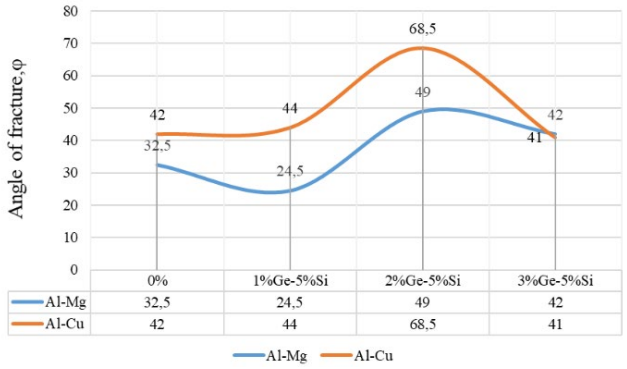


**Figure 6.** Graph of the dependence of the fracture angle φ on the germanium content in the sample

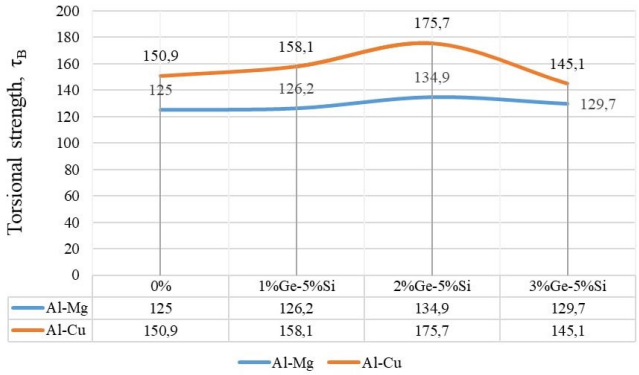


**Figure 7.** Graph of the dependence of the torsional strength $\tau_B$ on the germanium content in the sample

## 3.2. Microstructural analysis

The microscopic analysis of the samples was carried out using an AmScope microscope. The microstructure images of the samples are presented in Figures 8 and 9.

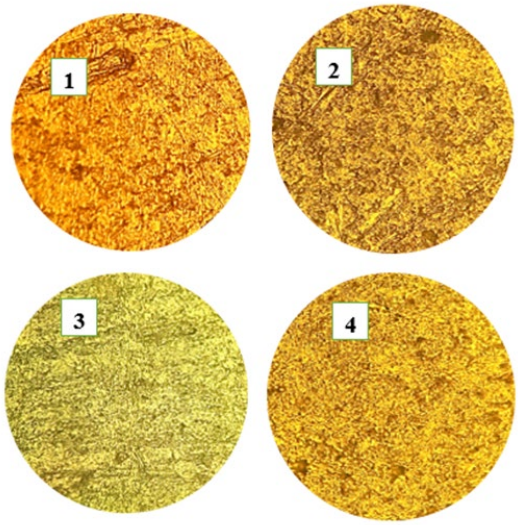


**Figure 8.** Microstructural image of the Al–Mg alloy:1-Al-Mg; 2-Al-Mg+0.1%Ge; 3-Al-Mg+0.2%Ge; 4-Al-Mg+0.3%Ge

The microstructural analysis of the Al–Mg alloy demonstrates that the addition of germanium oxide significantly alters the structure of the alloy. The observed microstructural changes are mainly characterized by dendrite refinement, more uniform phase distribution, and structural densification. As a modifying element, germanium affects the kinetics of solidification and promotes the formation of new nucleation sites during crystallization.

In the unmodified Al–Mg alloy (Figure 8.1), the microstructure exhibits relatively coarse and non-uniform features. The α-Al solid solution forms the primary matrix, while Mg-rich phases are concentrated in certain regions. A relatively large dendritic arm spacing is observed, indicating a slower solidification process. Under such conditions, phase segregation becomes more pronounced, which may result in non-uniform mechanical properties throughout the alloy.

In the sample containing 0.1% Ge (Figure 8.2), the reduction in dendrite size and the more homogeneous distribution of phases indicate the modifying effect of germanium. The addition of Ge increases the number of crystallization nuclei and accelerates the formation of new grains during solidification. When the Ge content reaches 0.2% (Figure 8.3), the structure becomes even finer and more dispersed. The phases are distributed very uniformly throughout the matrix, while the dendritic morphology is significantly reduced. In the sample containing 0.3% Ge (Figure 8.4), the microstructure appears to be the most homogeneous and compact among all investigated samples. The phases are finely dispersed and distributed almost uniformly throughout the entire volume of the alloy. The dendritic structure is substantially suppressed, and the matrix becomes more compact.

In the unmodified Al–Cu alloy (Figure 9.1), the structure is characterized by coarse and non-uniform dendrites, while Cu-rich eutectic phases are distributed irregularly within the α-Al solid solution matrix. Noticeable microstructural refinement was observed after the addition of 0.1% Ge (Figure 9.2). The dendrite size decreased and the distribution of phases became relatively more homogeneous. The addition of germanium increases the number of crystallization nuclei, resulting in the formation of new nucleation sites and consequently leading to dendrite refinement. At the same time, the continuous network-like morphology of Cu-rich intermetallic phases was reduced, and the structure became denser and more compact.

When the Ge content was increased to 0.2% (Figure 9.3), the modifying effect became more pronounced. The microstructure revealed a fine and dispersed distribution of eutectic phases, while the dendritic arm spacing decreased significantly. The refinement of intermetallic compounds restricts dislocation movement, which consequently improves the strength characteristics of the alloy. In addition, the formation of a more homogeneous structure contributes to the reduction of internal stresses.

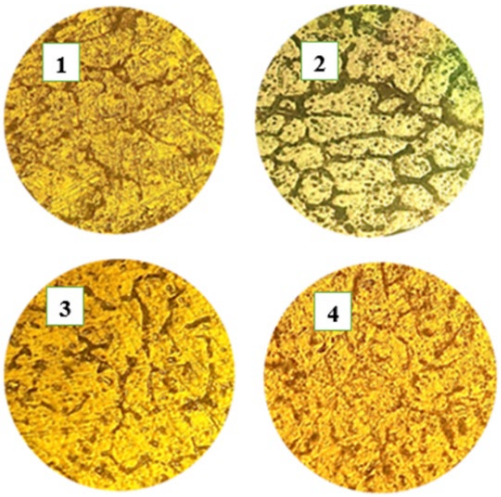


**Figure 9.** Microstructural image of the Al–Cu alloy:1-Al-Cu; 2-Al-Cu+0.1%Ge; 3-Al-Cu+0.2%Ge; 4-Al-Cu+0.3%Ge

In the sample containing 0.3% Ge (Figure 9.4), the microstructure exhibited the finest and most uniform morphology among all investigated samples. The dendritic structure was almost completely suppressed, and the eutectic phases were distributed in a very fine dispersed form. This indicates a strong modifying effect of germanium on the solidification process. Such structural refinement not only enhances the hardness and strength of the alloy, but also contributes to the reduction of casting defects. The uniform distribution of phases may improve diffusion processes and thereby enhance the service properties of the alloy.

As the Ge content increased, dendrites became finer, eutectic phases were dispersed more uniformly, and the overall structural homogeneity improved. The obtained results indicate that the addition of 0.2–0.3% Ge represents the optimum range for effective modification of the Al–Cu alloy.

## 3.3. Statistical Validation (ANOVA)

In this study, the one-way ANOVA was used to verify the reliability of the experimental tests. Three key assumptions that should be satisfied when applying one way analysis of variance. 1-The observations are obtained independently and randomly from the populations defined by the factor levels; 2-The population at each factor level is (approximately) normally distributed, and 3-These normal populations have a common variance. Paying attention to these assumption one-way ANOVA is designed, and following Table 3 and Table 4 shows the initial inputs. Minitab statistical software is used to analyze the data. For the accuracy of the experimental results, the repetitions was taken as three, the 95% (α=0.05) confidence level was chosen. Table 5 shows the results of experiments with the addition of Ge and Si modifier as an input factor to Al-Mg and Al-Cu alloys and the results of fracture angle and torsional strength tests of the samples obtained from these experiments. Each result was measured three times.

Table 3. ANOVA method

| | |
|---|---|
| Null hypothesis | All means are equal |
| Alternative hypothesis | Not all means are equal |
| Significance level | α = 0,05 |
| Equal variances were assumed for the analysis | |

Table 4. Factor Information for ANOVA

| Factor | Levels | Values |
|---|---|---|
| Ge% | 3 | 1%Ge; 2%Ge; 3%Ge |

Table 5. Experimental test results for ANOVA

| | **Al-Mg, $\varphi_1$** | **Al-Mg, $\varphi_1$** | **Al-Cu, $\tau_{B1}$** | **Al-Cu, $\tau_{B1}$** |
|---|---|---|---|---|
| 1%Ge+5%Si | 20,0 | 44,0 | 126,2 | 156,0 |
| 2%Ge+5%Si | 49,0 | 70,0 | 134,9 | 175,7 |
| 3%Ge+5%Si | 42,0 | 41,0 | 131,0 | 145,6 |
| 1%Ge+5%Si | 24,5 | 42,0 | 126,0 | 158,1 |
| 2%Ge+5%Si | 48,0 | 68,5 | 136,0 | 175,0 |
| 3%Ge+5%Si | 40,0 | 43,0 | 129,0 | 145,1 |
| 1%Ge+5%Si | 25,0 | 43,0 | 128,0 | 158,6 |
| 2%Ge+5%Si | 52,0 | 69,0 | 133,0 | 176,8 |
| 3%Ge+5%Si | 46,0 | 41,0 | 129,7 | 144,3 |

The results of the one-way ANOVA are presented in Table 6. It evaluates the effect of germanium content (Ge, %) on the fracture angle $\varphi$ and torsional strength $\tau_B$ of Al–Mg and Al–Cu alloys. The ANOVA results clearly demonstrate that the Ge content has a statistically significant influence on both investigated mechanical responses.

Table 6. Results of the analysis of variance

| **Source** | **DF** | **Adj SS** | **Adj MS** | **F-Value** | **P-Value** |
|---|---|---|---|---|---|
| | | ***Fracture angle of Al-Mg, $\varphi_1$*** | | | |
| Ge% | 2 | 1131,50 | 565,750 | 79,87 | 0,000 |
| Error | 6 | 42,50 | 7,083 | | |
| Total | 8 | 1174,00 | | | |
| | | ***Fracture angle of Al-Cu, $\varphi_2$*** | | | |
| Ge% | 2 | 1442,72 | 721,361 | 741,97 | 0,000 |
| Error | 6 | 5,83 | 0,972 | | |

| | | | | | |
|---|---|---|---|---|---|
| Total | 8 | 1448,56 | | | |
| | ***Torsional strength of Al-Mg, $\tau_{B1}$*** | | | | |
| Ge% | 2 | 94,842 | 47,421 | 31,29 | 0,001 |
| Error | 6 | 9,093 | 1,516 | | |
| Total | 8 | 103,936 | | | |
| | ***Torsional strength of Al-Cu, $\tau_{B2}$*** | | | | |
| Ge% | 2 | 1442,29 | 721,143 | 685,35 | 0,000 |
| Error | 6 | 6,31 | 1,052 | | |
| Total | 8 | 1448,60 | | | |

Ge content performs a noticeable effect, as evidenced by a high F-value of 79.87 for $\varphi_1$ of the Al–Mg alloy. The adjusted sum of squares associated with Ge (1131.50) accounts for the major portion of the total variability, while the error contribution remains minimal. This defines that variation in the content of Ge substantially modify the fracture behavior of the Al–Mg alloy. In addition, more pronounced effect of Ge is observed for $\varphi_2$ of the Al–Cu alloy. The extremely high F-value of 741.97, together with a P-value of 0.000, confirms that Ge content is the dominant factor governing the fracture angle in this alloy system.

Regarding the torsional strength of the Al–Mg and Al-Cu alloy ($\tau_{B1}$ and $\tau_{B2}$ respectively), the ANOVA results also indicate a statistically significant effect of Ge content (F-value of 31.29 and 685.35, P-value of 0.001 and 0.000 respectively). The dominance of the Ge factor and the small experimental error highlight the high sensitivity of the Al–Cu alloy's torsional strength to variations in Ge concentration.

According to the ANOVA results, the effect of Ge content is more pronounced in Al–Cu alloys than in Al–Mg alloys for both fracture angle and torsional strength. Furthermore, fracture angle responses exhibit higher sensitivity to Ge addition than torsional strength. These findings suggest that germanium plays a crucial role in altering the fracture mechanisms and strengthening behavior of aluminium-based alloys, particularly in Al–Cu systems.

To verify the validity of the ANOVA results and assess the adequacy of the developed statistical models, residual analyses were performed (Figure 8) shows the.

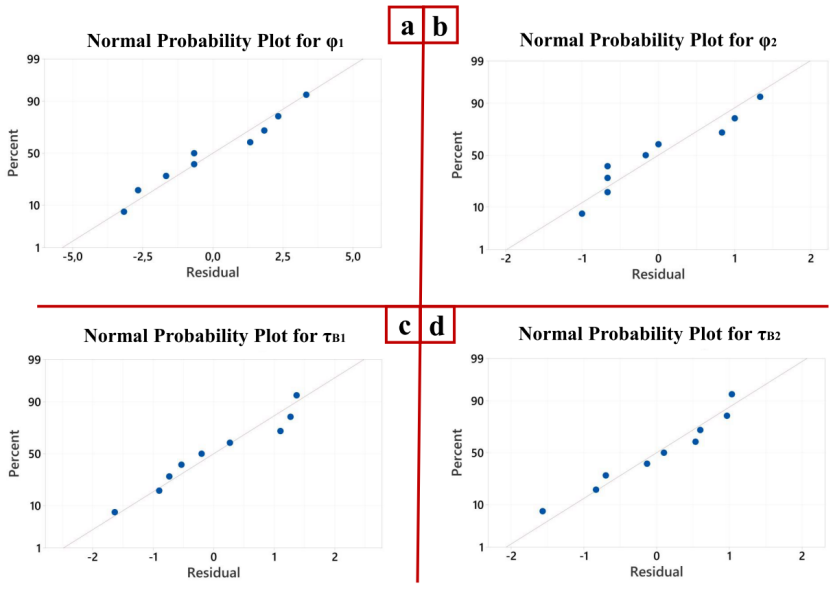


**Figure 8.** Normal probability plots of the residuals for (a) the fracture angle of Al–Mg alloy ($\varphi_1$), (b) the fracture angle of Al–Cu alloy ($\varphi_2$), (c) the torsional strength of Al–Mg alloy ($\tau_{B1}$), and (d) the torsional strength of Al–Cu alloy ($\tau_{B2}$)

These plots are used to assess the normality assumption of the residuals, which is a key requirement for the validity of the ANOVA results. As shown in Fig. 8(a) and Fig. 8(b), the residuals corresponding to the fracture angle of the Al–Mg and Al–Cu alloys ($\varphi_1$ and $\varphi_2$ respectively) are distributed closely along the reference straight line, with only minor deviations at the tails. The data points align well with the normal probability line, demonstrating good agreement with the normality assumption. The relatively narrow spread of residuals further confirms the high experimental consistency for this response. Moreover, Fig. 8(c) and Fig. 8(d) present the normal probability plots for

the torsional strength of Al–Mg and Al–Cu alloys ($\tau_{B_1}$ and $\tau_{B_2}$, respectively). In both cases, the residuals show a linear pattern with no systematic curvature or clustering, indicating that the error terms are normally distributed.

The graph performed in Figure 8 confirms that the residuals for all four responses are approximately normally distributed. Therefore, the assumptions underlying the ANOVA are satisfied, and the statistical conclusions regarding the significant effect of Ge content on fracture angle and torsional strength are reliable.

Regression models are essential analytical tools that measure relationships between variables, enabling precise forecasting, predictive analysis, and data-driven decision-making across various industries. They assess the significance of predictors, project future trends, and identify key drivers, helping businesses optimize strategies, minimize risks, and gain competitive edges. Therefore, it is important to develop regression equations of the results obtained from this research work.

## 3.4. Predictive Digital Models

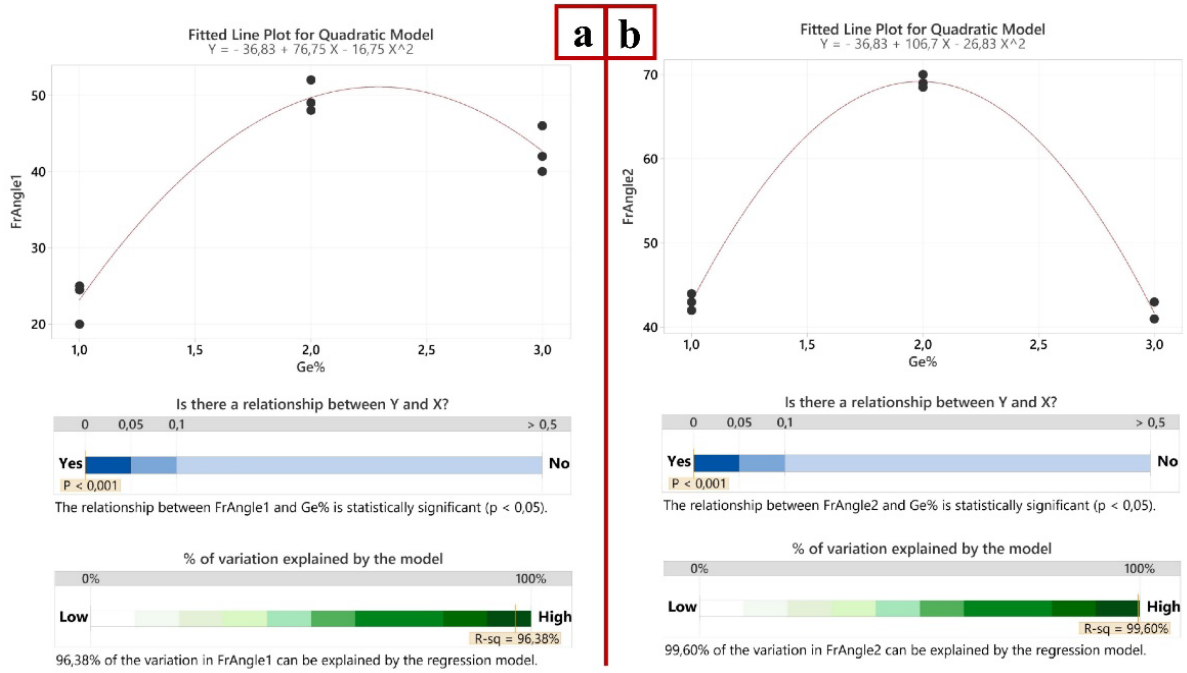


**Figure 9.** Fitted line plots of the fracture angle φ vs the Ge content. a) Al-Mg specimens, b) Al-Cu specimens

Fig. 8 shows and analyzes the quadratic regression model of the influence of Ge content on the fracture angles $\varphi_1$ and $\varphi_2$ in Al-Mg and Al-Cu alloys. In both cases, a high correspondence is observed between the experimental points and the regression curve. This indicates the nonlinear (parabolic) influence of Ge content on the response variables. The dependence of fracture angle on Ge content is expressed by the quadratic equation Eq.1 for Al-Mg and Eq.2 for Al-Cu.

$$\varphi_1=-36.83-16.75x^2+76.75x \quad (1)$$

$$\varphi_2=-36.83-26.83x^2+106.7x \quad (2)$$

In this case, $\varphi_1$ and $\varphi_2$ values reach their maximum values around Ge% ≈ 2%. In addition, at low (1%) and high (3%) concentrations, a moderate decrease in $\varphi_1$ and a sharp decrease in $\varphi_2$ are observed. The statistical significance of the model is very high, since $p<0.001$, i.e., Ge% has a significant influence on $\varphi_1$ and $\varphi_2$. The coefficient of determination for $\varphi_1$ and $\varphi_2$ are $R_1$=96.38% and $R_2$=99.60%, respectively. This indicates a very high reliability of these digital models. Furthermore, from the prediction plots of the fracture angle φ versus Ge content shown in Figure 10, it can be seen that most of the experimental points are located within the prediction interval.

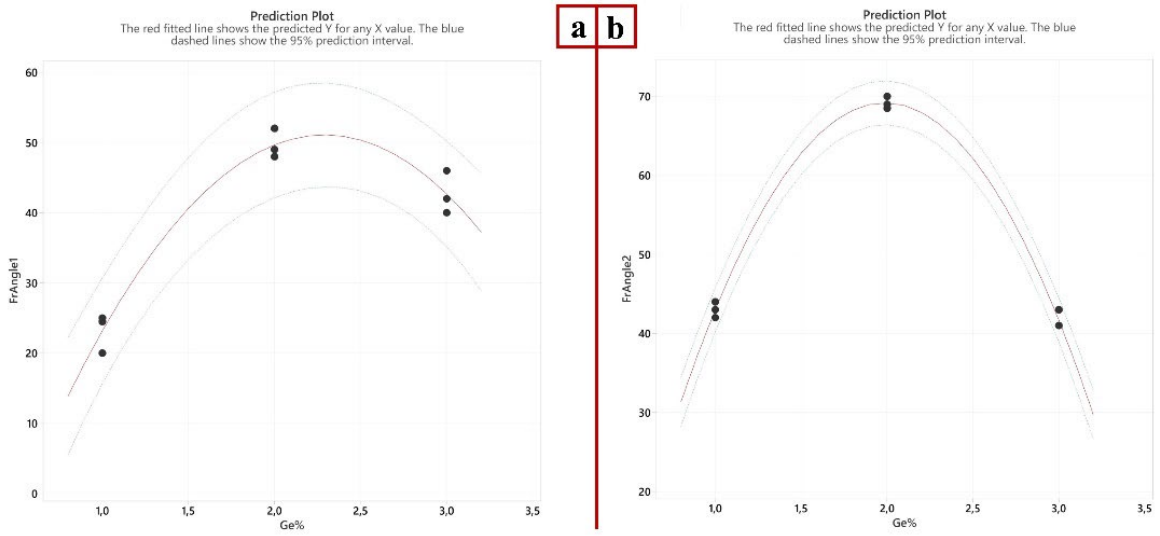


**Figure 10.** Prediction plots of the fracture angle "φ" vs the Ge content. a) Al-Mg specimens, b) Al-Cu specimens

In Fig. 10, the red line represents the predicted values based on regression models, and the blue dotted lines represent the 95% prediction interval. At Ge%≈2%, the interval narrows, i.e., the model's accuracy is highest in this region. At extreme values (1% and 3%), the uncertainty of the forecast increases. This once again confirms the existence of the optimal operating range of Ge%.

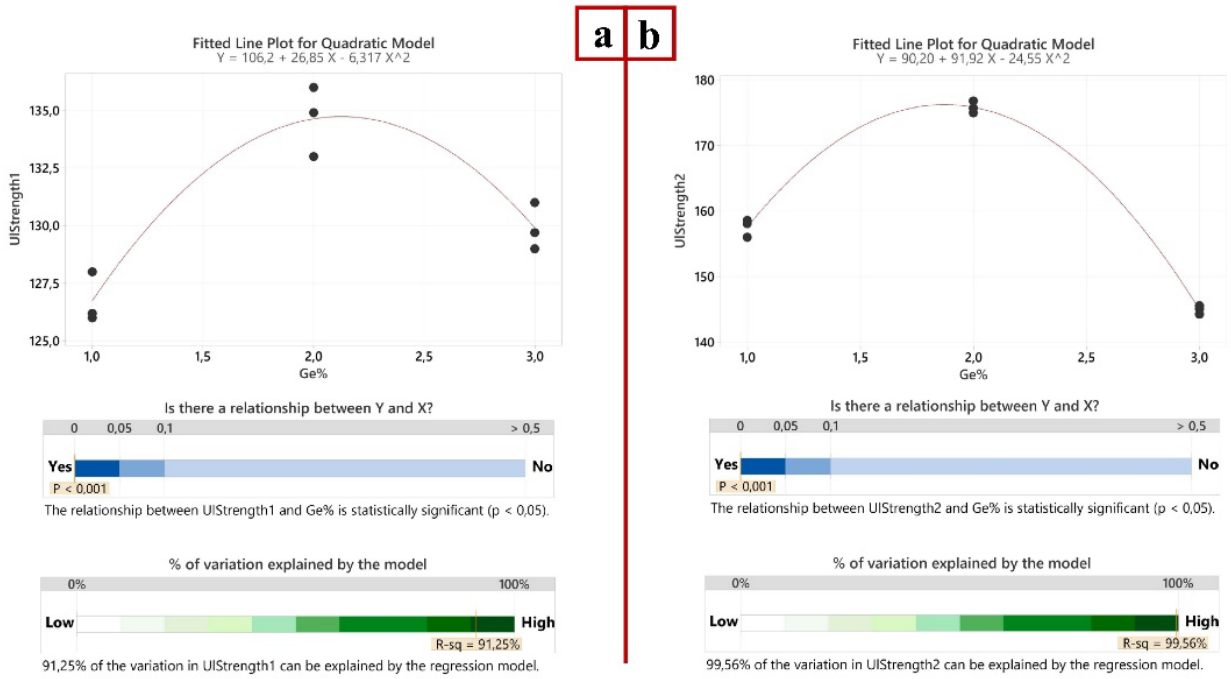


**Figure 11.** Fitted line plots of the torsional strength vs the Ge content. a) Al-Mg specimens, b) Al-Cu specimens

In Fig. 11, the influence of the Ge concentration on the torsional strengths of Al-Mg and Al-Cu alloys $\tau_{B1}$ and $\tau_{B2}$ (UlStrength1 and UlStrength2, respectively) is estimated using the developed quadratic regression model. For both response indicators, a parabolic relationship with Ge content is observed. The regression equations for $\tau_{B1}$ and $\tau_{B2}$ are expressed as follows (Eq.3 and Eq.4):

$$\tau_{B1}=106.2+26.85x-6.317x^2 \quad (3)$$

$$\tau_{B2}=90.2+91.92x-24.55x^2 \quad (4)$$

The values of $\tau_{B1}$ and $\tau_{B2}$ also reach their maximum values around Ge%≈2%. A relatively low trend is observed in 1%, and a decrease in 3%. Statistical analysis shows that this relationship is highly significant ($p<0.001$). The coefficients of determination of the $\tau_{B1}$ and $\tau_{B2}$ models are R2 = 91.25% and R2 = 99.56%, respectively. That is, the main part of the changes in τB1 and τB2 is explained by Ge%. Figure 12 shows the prediction plots of the developed digital models. From the graphs created using the Minitab program, it can be seen that most of the experimental points are located within the prediction interval.

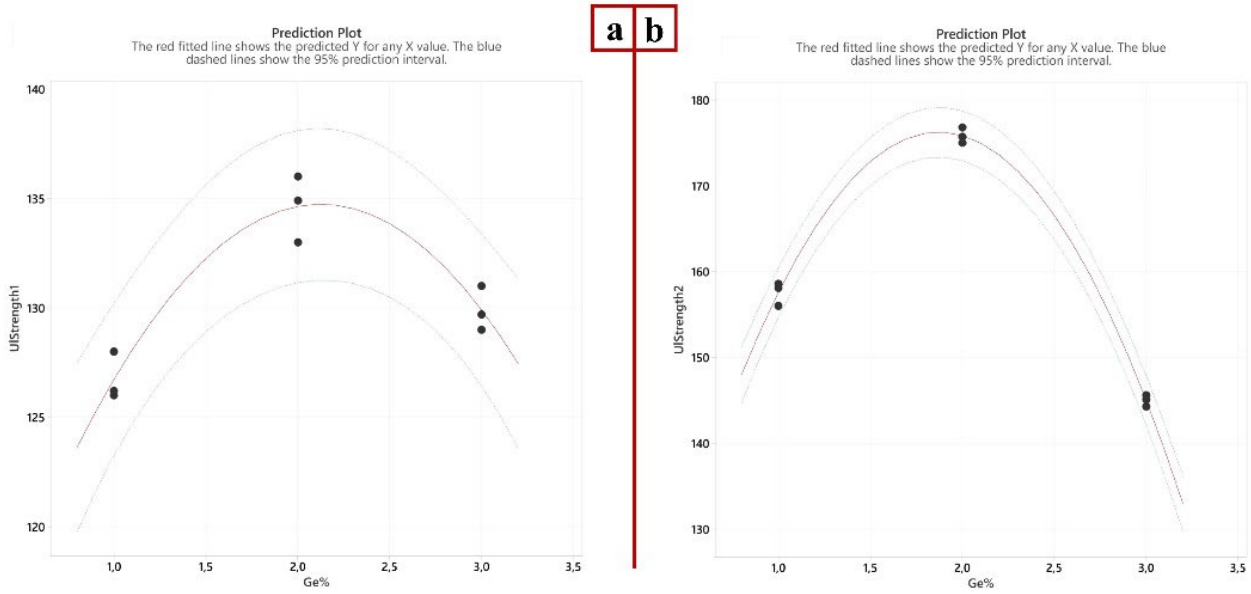


**Figure 12.** Prediction plots of the torsional strength vs the Ge content. a) Al-Mg specimens, b) Al-Cu specimens

The results demonstrate a strong quadratic relationship between Ge concentration and both $\varphi_1$ and $\varphi_2$. In both cases, the responses increase with Ge percentage up to an optimal value of approximately 2%, beyond which a decline is observed. Statistical analysis confirms the significance of the models ($p < 0.001$), with high coefficients of determination ($R^2$ = 96.38% for $\varphi_1$ and 99.60% for $\varphi_2$). The prediction plots further validate the reliability of the developed models, indicating that Ge% around 2% represents an optimal operating condition for maximizing the fracture angle responses. In addition, a pronounced quadratic relationship between Ge concentration and both $\tau_{B1}$ and $\tau_{B2}$ are also developed. In both cases, the mechanical strength increases with Ge modifier up to an optimal concentration of approximately 2%, after which a decline is observed. Statistical analysis confirms the significance of the developed models ($p < 0.001$), with high coefficients of determination ($R^2$ = 91.25% for $\tau_{B1}$ and 99.56% for $\tau_{B2}$). These findings suggest that excessive Ge content adversely affects the mechanical performance, highlighting the importance of optimizing Ge% concentration.

## 3.5. Discussions

The obtained results differ in several aspects from previously reported studies on the modification of Al-Cu and Al-Mg alloys with germanium. In most earlier investigations, Ge was mainly studied as a modifier for silicon-containing aluminum alloys [19], whereas in the present work the microstructural influence of Ge on both Al-Cu and Al-Mg systems was comprehensively evaluated. The experimental results demonstrated that the addition of germanium led to significant grain refinement, dispersion of eutectic and intermetallic phases, and improvement in structural homogeneity. In particular, the finest and most uniformly distributed phases were observed within the 0.2–0.3% Ge range. Such structural refinement is considered an important factor for enhancing the mechanical properties of the alloys. The distinctive feature of this research lies in the comparative investigation of the modifying effect of germanium in two different aluminum-based alloy systems and in determining the optimum Ge content.

Obtained results show that the increase in Ge content improves the strength and microstructural refinement only up to a certain limit; however, above 0.2% Ge, the effectiveness gradually decreases and, in some cases, deterioration of the mechanical properties may occur. The main reason for this behavior is associated with the limited solubility of germanium in the aluminum matrix. When the Ge concentration exceeds the optimal level, excessive intermetallic compounds and undissolved particles are likely to form. These particles tend to accumulate along grain boundaries during solidification, leading to the formation of brittle phases. Furthermore, oxidation of Ge-containing compounds may promote slag formation in the melt, which decreases the purity of the alloy and increases the number of internal defects. Slag inclusions and coarse

intermetallic phases act as stress concentrators, disturbing dislocation movement and consequently reducing the ductility and strength of the alloy.

The obtained results are also of considerable industrial significance. Germanium-modified Al-Cu and Al-Mg alloys possess enhanced strength, improved wear resistance, and superior service properties, making them promising materials for aerospace, automotive, and mechanical engineering applications. Al-Cu alloys can be effectively used for heavily loaded structural components, whereas Al-Mg alloys are highly suitable for lightweight and corrosion-resistant structures. By controlling the microstructure through Ge modification, it becomes possible to extend the service life of the alloys, improve machining quality, and reduce casting defects. Consequently, this approach may contribute to increased manufacturing efficiency and reduced material consumption.

## 4. Conclusions

Test results on samples showed that the addition of germanium (Ge) and silicon (Si) to an aluminium-magnesium alloy had a positive effect on its torsional strength. According to experimental tests and digital analysis, following conclusions can be drawn.

Germanium content of 1–2%, a 6–8% increase in sample strength was observed. However, with further increases in germanium content, its solubility in the alloy decreased and slag formation increased, leading to a reduction in torsional strength. A similar trend was observed in Al-Cu alloys. The maximum torsional strength was obtained at a germanium content of up to 2%. However, a further increase in the amount of germanium above 2% led to a reduction in the torsional strength of the alloys.

This study systematically investigated the effect of Ge% concentration on fracture angle and mechanical strength parameters of ZL201 and AA5056 aluminium alloy using quadratic regression modeling. The results clearly demonstrate that Ge plays a critical role in governing both frictional and mechanical responses, exhibiting a pronounced nonlinear behavior.

For all investigated responses, the values increased with Ge up to an optimal concentration of approximately 2%, beyond which a consistent decline was observed. Statistical analysis confirmed the high significance of the developed models ($p < 0.001$), with excellent goodness of fit ($R^2$ ranging from 91.25% to 99.60%), indicating that the quadratic models reliably describe the experimental behavior.

Overall, the findings highlight the existence of a well-defined optimal Ge% concentration around 2%, at which both frictional and mechanical properties are maximized. These results emphasize the importance of precise control and optimization of Ge% concentration in practical applications and provide valuable guidance for the design and optimization of systems where fracture failure and torsional strength performance are critical.

## References


[1] J. Yang, B. Liu, and H. Huang. Research on composition-process-property prediction of die casting Al alloys via combining feature creation and attention mechanisms. J. Mater. Res. Technol., vol. 28, 2024. doi: 10.1016/j.jmrt.2023.11.257.

[2] T. Soto, I. Alfonso, F. González, C. Aguilar, L. Béjar, I. A. Figueroa, J. Vargas, M. Abatal, and F. H. Samuel. An overview on the identification and characterization of Cu-rich second phases in casting Al alloys. Int. J. Metalcast., vol. 17, no. 3, 2023. doi: 10.1007/s40962-022-00889-4.

[3] S. Shahria. Optimization of molding sand composition for casting Al alloy. Int. J. Mech. Eng. Appl., vol. 5, no. 3, 2017. doi: 10.11648/j.ijmea.20170503.13.

[4] J. Gao, J. Zhong, G. Liu, S. Zhang, J. Zhang, Z. Liu, B. Song, and L. Zhang. Accelerated discovery of high-performance Al-Si-Mg-Sc casting alloys by integrating active learning with high-throughput CALPHAD calculations. Sci. Technol. Adv. Mater., vol. 24, no. 1, 2023. doi: 10.1080/14686996.2023.2196242

[5] Q. Zheng, B. Zhang, T. Chen, and J. Wu. Achieving superior grain refinement efficiency for Al–Si casting alloys through a novel Al–La–B grain refiner. J. Mater. Res. Technol., vol. 30, 2024; doi: 10.1016/j.jmrt.2024.03.070.

[6] S. Tursunbaev, N. Turakhodjaev, L. Zhang, Z. Wang, U. Mardonov, & M. Saidova. Mechanical properties and evolution of the microstructure of Al-Cu-Mg system alloys under the influence of alloying elements (Ge and Si). International Journal of Mechatronics and Applied Mechanics. 2024; 2024(18), 164–169. https://doi.org/10.17683/ijomam/issue18.19

[7] F. Zhang, D. Shi, Z. He, X. Wang, L. Li, Z. Zhan, and Z. Yuan. Precipitated phase characteristics and fracture behaviour of cast Al–Cu–Mn alloy. J. Mater. Res. Technol. 2023; vol. 25, pp. 2815–2825.

[8] S. Tursunbaev, N. Turakhodjaev, S. Mardonakulov & S. Toshmatova. Effect of germanium oxide on the properties of aluminum casting details in agricultural machinery. BIO Web of Conferences. 2024; 85. https://doi.org/10.1051/bioconf/20248501024

[9] M. Tiryakioğlu, J. Robinson, M. Salazar-Guapuriche, Y. Zhao, and P. Eason. Hardness-strength relationships in the aluminum alloy 7010. Mater. Sci. Eng. A. 2015; vol. 631, pp. 196–200. doi: 10.1016/j.msea.2015.02.049.

[10] W. Li, K. Chen, H. bin Jiao, L. Zhou, Z. Yang, and S. Chen. Effect of trace germanium on microstructure and quenching sensitivity of 7056 aluminum alloy. Cailiao Gongcheng/ J. Mater. Eng. 2019; vol. 47, no. 3. doi: 10.11868/j.issn.1001-4381.2018.000624.

[11] M. Riglos, M. de la Cruz, and A. Tolley. Accelerated age hardening by plastic deformation in Al–Cu with minor additions of Si and Ge. 2011; Scripta Mater., vol. 64, no. 2, pp. 169–172.

[12] S. Gulov, I. Ganiev, A. Berdyaev, R. Saidzoda, and D. Ashurmatov. The influence of germanium and strontium on the microstructure and mechanical and technological properties of the AK9M2 alloy. Bull. South Ural State Univ. Ser. Metall. 2019; vol. 19, no. 1, pp. 50–58.

[13] Y. Gong, J. Gu, S. Ni, H. Wu, & M. Song. A good combination of strength and ductility of ultra-coarse-grained Cu-Al alloy with coarse-grained surface layer via

pre-torsional treatment. Micron. 2020; 129. https://doi.org/10.1016/j.micron.2019.102783

[14] Y. Lei, L. Jin, D. Li, H. Zhu, & X. Du. Comparison of torsional damage and size effects of BFRP- and steel-reinforced concrete beams with different stirrup ratios. Engineering Structures. 2023; 285. https://doi.org/10.1016/j.engstruct.2023.116042

[15] T. Sarvar, T. Nodir, U. Mardonov, B. Saydumarov, D. Kulmuradov, & M. Boltaeva. Effects of germanium (Ge) on hardness and microstructure of Al-Mg, Al-Cu, Al-Mn system alloys. International Journal of Mechatronics and Applied Mechanics. 2024; 2024(16), 179–184. https://doi.org/10.17683/ijomam/issue16.21

[16] M. Umidjon, T. Oybek, A. Khusniddin, & T. Sarvar. Mathematical approach to the flank wear of high-speed steel turning tool in diverse external cutting environments. International Journal of Mechatronics and Applied Mechanics. 2023; 2023(14), 19–26. https://doi.org/10.17683/ijomam/issue14.3

[17] X. Ye, W. Su, Y. Chen, H. Cheng, & L. Xiao. Strengthening 5A02 Al alloy via gradient structures processed by severe torsional deformation. Materials Today Communications. 2023; 36. https://doi.org/10.1016/j.mtcomm.2023.106745

[18] M. Setkit, T. Imjai, U. Chaisakulkiet, R. Garcia, K. Dangyem, K. Sanupong, & W. Chamnankit. Torsional strengthening of low-strength rc beams with post-tensioned metal straps: An experimental investigation. Walailak Journal of Science and Technology. 2020; 17(12). https://doi.org/10.48048/wjst.2020.11908

[19] R. Bjørge, D. Marioara, S. Andersen, & R. Holmestad. Germanium network connecting precipitates in an Mg-rich Al–Mg–Ge alloy. Journal of electron microscopy. 2010; 59(S1), 129-133.